analytical chemistry

Letter

pubs.acs.org/ac

MALDI Mass Spectrometry Imaging in Microscope Mode with Infrared Lasers: Bypassing the Diffraction Limits

Jens Soltwisch,[†,§] Guido Göritz,[‡] Julia H. Jungmann,[†,∥] András Kiss,[†] Donald F. Smith,[†] Shane R. Ellis,[†] and Ron M.A. Heeren*[,†]

[†]FOM Institute AMOLF, Science Park 104, 1098 XG Amsterdam, The Netherlands

[‡]GWU Lasertechnik, D-50374 Erftstadt, Germany

Supporting Information

ABSTRACT: This letter demonstrates the use of infrared matrix-assisted laser desorption/ionization coupled with microscope mode mass spectrometry imaging. It is aimed to explore the use of intrinsic water in tissue as a matrix for imaging at spatial resolutions below the diffraction limit of the employed IR optics. Stigmatic ion optics with a magnification factor of ∼70 were used to project the spatial distribution of produced ions onto a detector while separating ions with different mass-to-charge ratios using a time-of-flight mass spectrometer. A pixelated detector was used to simultaneously record arrival time and impact position. A previously described dried-droplet sample system of 2,5-dihydroxybenzoic acid (DHB) and 5 peptides covered by a copper grid for defined surface structure was used to benchmark the light- and ion-optical setup for spatial resolution and mass spectrometric performance. A spatial resolving power of 9.8 μm, well below the optical limit of diffraction (14 μm for the given setup), was established. After, frozen cryosections from a biological model system were measured by exploiting the endogenous water content as a matrix. Principal component analysis enabled a clear distinction between distinct tissue regions identified by both light microscopy and MS imaging.

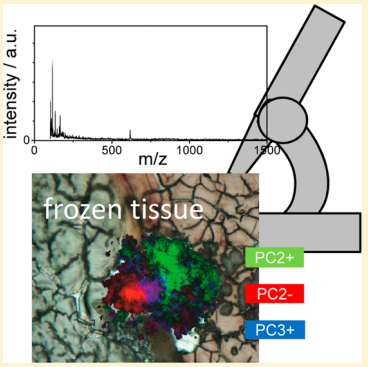

Matrix-assisted laser desorption/ionization-mass spectrometry imaging (MALDI-MSI) provides microscopic "images" of the spatial distribution of compounds in complex organic samples such as thin slices of biological tissue. The sample is typically treated with a chemical matrix and irradiated with laser pulses of a few nanoseconds duration that initiates material desorption. The matrix is chosen to both absorb the laser light and to concomitantly ionize codesorbed analyte during the process of material ejection. In the majority of cases, the so-called microprobe approach is used for MSI experiments, where mass spectra are acquired from small areas on the sample surface pixel-by-pixel.[1,2] The information from these mass spectra is subsequently merged together with the respective spatial coordinates to form a mass spectrometric image with a spatial resolution that is largely defined by the size of the laser spot. While impressive improvements have been made regarding the miniaturization of the laser spot size in ultraviolet (UV) MALDI-MSI,[3] the spatial resolution is ultimately limited by the optical diffraction limit. Furthermore, in UV-MALDI-MSI, a homogeneous coating of the sample with matrix is a key factor requirement for a successful analysis. The applied matrix solution has to interact with the material such that analyte molecules are extracted and ultimately cocrystallized with the matrix,[4] while at the same time, its application must minimize analyte delocalization on the surface.

As an alternative to desorption/ionization with UV-light, MALDI using infrared (IR) lasers commonly emitting at wavelengths around 3 μm have been employed.[5] This wavelength overlaps strongly with the OH-stretch vibration and enables the use of endogenous water invariably present in biological samples as a matrix, thereby avoiding the application of an "external" chemical matrix.[6−8] However, microscope mode MSI (see below) requires a high vacuum ion source to prevent deviations of the ion paths due to random collisions with background gases. In order to use water as a matrix under these high vacuum conditions, evaporation has to be prevented. Therefore, the hydrated sample must be frozen and kept sufficiently cooled within the instrument.[6] In an approach demonstrated by Pirkl et al., for a fine vacuum ion source (∼1 mbar), the sample holder and target plate were cooled with liquid nitrogen to temperatures of ∼150 K.[6] However, since the diffraction limit ultimately defines the achievable laser focus, the utility of IR-MALDI is severely hampered in the high-resolution microprobe MALDI-MSI. So far, spot sizes as small as ∼30 μm have been reported using separated spots of a focused IR-laser beam and a resolution of 40 μm has been achieved with oversampling.[9,10] In a similar approach, plant material was investigated with focused 40 μm IR-laser spot diameter when employing laser ablation electrospray ionization.[11]

As an alternative to the scanning probe scheme, microscope mode MALDI-MSI has been developed.[12] In this setup, a relatively large sample area (e.g., a spot of 150−300 μm

Received: October 21, 2013
Accepted: December 5, 2013

dx.doi.org/10.1021/ac403421v | *Anal. Chem.* XXXX, XXX, XXX−XXX

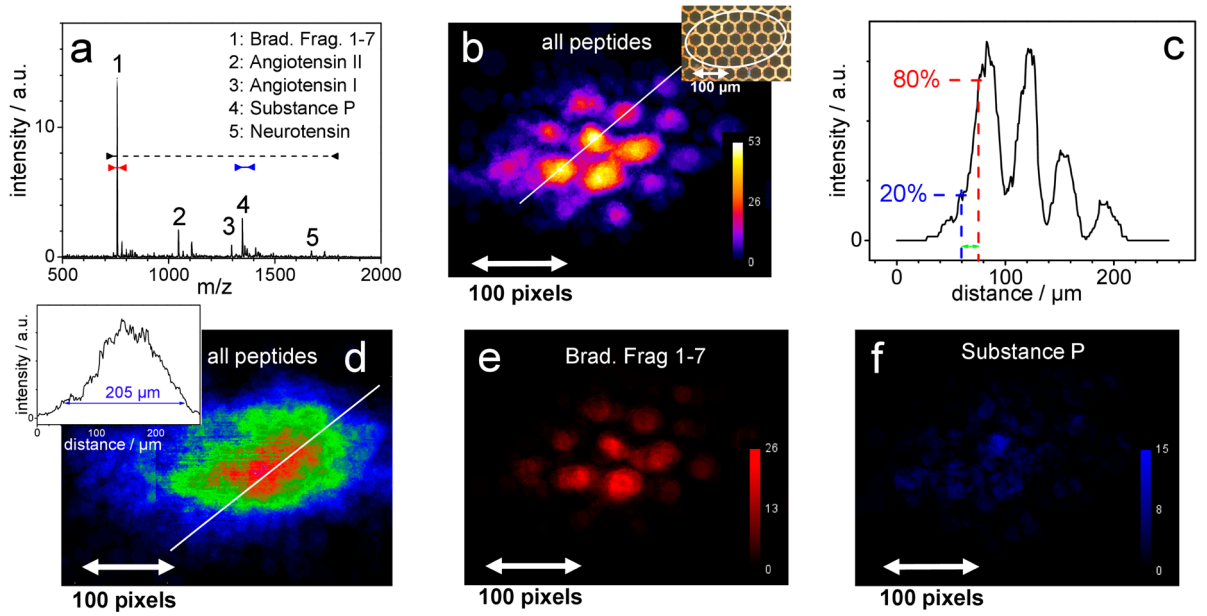

Figure 1. (a) IR–MALDI integrated mass spectrum of a peptide mix with DHB over all detector pixels and 500 laser shots on a fixed position. (b) Spatial distribution of all peptide ion signal intensities on the detector summed over 500 shots. (c) Intensity line scan, as indicated by the white line in (b). (d) Spatial distribution of all peptide ion signal intensities on the detector summed over 500 shots from 500 different positions of the sample. Inset in (d), intensity line-scan, as indicated by the white line in (d). (e and f) Spatial distribution of the ion signal of (e) bradykinin fragments 1–7 and (f) substance P on the detector extracted from the data set shown in (a and b).

diameter) is uniformly irradiated and the resulting ion cloud is ion-optically magnified and imaged onto a position-sensitive detection system. In addition to the flight time of the ions that are related to the ions m/z, the detector simultaneously records the impact coordinates of ions on its surface. The lateral resolution is now defined only by the pixel size of detector and the quality of the ion-optical system that possesses a much lower (ion-optical rather than light-optical-based) diffraction limit. Thus, the optical diffraction limit no longer determines spatial resolution. Recently, a new detector system for this type of setup based on the Timepix technology[13] has been introduced to be capable of delivering both high spatial and mass resolution[14] and also of detecting high masses above 400 kDa.[15] Using a mass microscope based on a triple focusing time-of-flight (TRIFT) mass spectrometer and this new detection system, pixels as small as 740 nm in diameter could be resolved in UV-MALDI and secondary-ion mass spectrometry (SIMS) measurements.[14,16−19] With the use of this instrument, Luxembourg et al. and others have demonstrated spatial resolutions as low as 4 μm, using both IR-MALDI-MSI and UV-MALDI-MSI.[20] Importantly, the 4 μm resolution achieved with IR-MALDI was below the optical diffraction limit of the IR-optical setup. In this previous work, succinic acid was applied as a matrix, and an MCP/phosphor screen assembly was employed as a spatially resolved detection system. However, limitations of the phosphor screen only allowed acquisition of either a total ion image, or an image of a selected, pretargeted mass region by blanking out all other ions. Herein, the coupling of IR-MALDI with a Timepix active pixel detector[13] is shown for the first time with the ability to acquire high spatial resolution microscope mode IR-MALDI images of multiple m/z values simultaneously.

EXPERIMENTAL SECTION

Experimental setup. All mass spectrometric work of this study was carried out on a TRIFT II instrument (Physical Electronics Inc., Chanhassen, MN). Ion optical lenses and three electrostatic sectors guiding the ions on their flight path allow for the stigmatic imaging of the produced, time-of-flight separated ion cloud onto the detector (see Figure 1a of the Supporting Information). The instrument is equipped with a combined microchannel-plate (MCP) and Timepix-based detection system, as previously described by Jungmann et al.[21] The detector is similar to the commercially available IonPix system (Omics2Image, Amsterdam, The Netherlands). This detector provides an array of 512 × 512 pixels that records both the flight times of ions in a time-to-digital manner (single stop TDC; 16 ns bin width) together with their respective impact coordinates on the detector surface. The dedicated "Pixelman" software package was used for chip control and data acquisition.[22] The ion optical setup and detection scheme were identical to the work of Jungmann et al. and Kiss et al.[18,21] The TRIFT instrument provides a liquid-nitrogen-fueled cooling stage and the necessary equipment to transfer and analyze frozen samples at ca. 150 K.

A Nd:YAG (Quanta-Ray INDI, Spectra Physics, Santa Clara, CA) pumped KTP-OPO (alphaScan with integrated versaScan-L 1064, GWU-Lasertechnik, Erftstadt, Germany) with a pulse duration of 5 ns at 20 Hz was used as a light source. The wavelength range was tunable from 2.7 to 3.1 μm. At 2.94 μm maximum pulse energy was measured at ∼15 mJ with less than 5% shot-to-shot variation. Due to the oscillator geometry and nonlinear effects within the OPO, the output beam contains a large number of laser modes. The beam profile is therefore initially inhomogeneous.

After tunable attenuation with an angle-sensitive dielectric mirror, laser-light was coupled into an 80 cm long hollow waveguide (HWG) (HWEA500850, Polymicro, Lisle, IL) with an inner diameter of 500 μm. The end surface of the HWG was imaged onto the sample surface within the TRIFT II. The use of telescope optics with a diminution of ca. 3:1 resulted in an elliptical spot of ca. 150 × 300 μm on the sample, as measured

dx.doi.org/10.1021/ac403421v | Anal. Chem. XXXX, XXX, XXX–XXX

by burn patterns on thermographic paper. All lenses and the vacuum window were either made of CaF_2 or infrared grade quartz (Infrasil). To achieve homogeneous energy distribution within the complete laser-spot, a flat top beam profile exiting the fiber was desirable. Therefore, a ball-bed microbending unit was employed to ensure sufficient mode mixing in the relatively short HWG.[23] To randomize the fine structure on the resulting near flat top profile over a number of shots, the fiber was softly shaken during measurements using a fan[24] (see Figure 1b of the Supporting Information). In order to avoid detector saturation, the laser fluence was adjusted to values slightly above the threshold for ion production.

Sample Preparation. A dried droplet preparation of 2,5-dihydroxybenzoic acid (DHB) was employed.[25] A binary matrix preparation with glycerol as an additive was chosen for good spatial homogeneity, as previously described.[26] The matrix was mixed 1:1 (v:v) with an aqueous solution of a peptide mixture containing bradykinin fragment 1−7 [average molecular weight (avg MW): 756.9 g/mol], angiotensin II (avg MW: 1046.2 g/mol), angiotensin I (avg MW: 1296.5 g/mol), substance P (avg MW: 1347.6 g/mol), and neurotensin (avg MW: 1672.9 g/mol) at a concentration of 0.4 mM each. An aliquot of 2 μL of the mix was pipetted onto a stainless steel target and allowed to dry under a stream of nitrogen. After the described gel-like film had developed,[26] the preparation was covered with a copper grid (hexagonal pattern, pitch of 36.3 and 8 μm thin bars (Agar Scientific, Stansted, U.K.) for a well-defined structure (Figure 1b inset). The preparation was then placed into the vacuum of the instrument and allowed to crystallize.

Fourteen micrometer thick cryo-sections of a bait fish (European smelt, *Osmerus eperlanus*) were prepared using a cryomicrotome (HM525, Microm, Walldorf, Germany) and thaw mounted onto polished silicon wafers (500 μm thick). Other substrate materials such as aluminum, indium tin oxide, or gold-coated glass slides produced a strong background signal in IR−MALDI experiments. Samples were placed in a rough vacuum and desiccated for 5 min to remove surface water. For analysis, the silicon slide was mounted onto a dedicated sample holder and dipped into liquid nitrogen for 2 min. Transfer into the mass spectrometer was performed under dry nitrogen atmosphere to prevent frost build up. The sample was held at a low temperature within the instrument by a liquid-nitrogen-fueled coldfinger. Light microscopy images were taken before and after MS measurement using a microscope (DMRX, Leica, Wetzlar, Germany) equipped with a digital camera (DXM1200, Nikon, Tokyo, Japan).

Safety Considerations. The employed laser is of laser safety class 4. Protective goggles have to be worn when working with free beams of such lasers.

RESULTS AND DISCUSSION

Figure 1 shows the results of experiments using the DHB preparation. Five-hundred shots, sufficient to ablate the whole sample spot, were summed to produce the resulting image. Figure 1a shows the integrated mass spectrum acquired over all pixels of the detector. Ions with m/z-values below 250 were not detected through the use of an appropriate acquisition start delay of the detector. Protonated and sodiated peptide ions constitute the most abundant peaks, with protonation being predominant. The mass resolution (mass/Δmass) in the peptide m/z-region is ca. 300. Figure 1b shows the spatial distribution of the signal intensity of the whole peptide mass region (marked with a black dashed line in Figure 1a) on the detector. The stigmatic imaging of the distribution of the peptide ion signals from the sample surface is clearly observed (as evidenced by the grid structure in the image). To determine the area on the sample imaged onto one pixel of the detector, line-scans (e.g., white line in Figure 1b) of the intensity image were analyzed. With the use of the known pitch of the grid, the pixel size was determined to be approximately 766 × 766 nm. This is in line with results from similar experiments employing UV-MALDI and SIMS.[14,18] The spatial resolving power can be defined by the distance between points of 80% and 20% of the slope height on a feature representing a sharp edge or step.[27] Averaging over several such features in Figure 1b reveals the spatial resolving power to be 9.8 ± 2.5 μm. Due to a different ion optical magnification setting, this value is higher than the 4 μm reported by Luxembourg et al.[20] Nonetheless, it lies well below the theoretical limit of diffraction of the employed IR-optics of 14 μm, as previously determined for an identical focusing lens.[20] Besides uncertainties in adjusting various components of the ion optical system, a potentially limiting factor for the spatial resolving power in microscope mode IR-MALDI-MSI is the velocity spread in the IR-MALDI-plume. Comparable to (wavelength dependent) chromatic aberration in light optics, the focal lengths of the employed ion optics show a dependence on kinetic energy. To minimize this effect, an energy slit placed in an intermediate focal plane can be used to reduce the spread (see Figure 1a of the Supporting Information). Since a narrow slit will greatly reduce ion counts reaching the detector, a compromise between desired spatial resolution and mass spectrometric sensitivity has to be found.

The overall laser spot size and homogeneity of measured ion signal within the laser spot was determined by integrating over 500 different positions on the grid, thereby averaging out the grid structure and possible inhomogeneity within the matrix preparation (Figure 1d). With the utilization of line scans, the elliptical spot size was measured to be 157 × 301 μm ($1/e^2$ definition). An ideal flat top ion signal intensity distribution was not achieved. Nonetheless, the intensity profile (inset in Figure 1d) shows a region of fairly constant high ion signal intensity in the center of the spot (~100 μm diameter) with rather steep flank regions to either side (~50 μm each).

Although all peptides were prepared at the same concentration, different ion signal intensities are observed. While a bias based on peptide sequence is expected, the effect is overlaid by a positive discrimination toward smaller masses that is a result of the single-stop TDC detection scheme. Any pixel hit by an earlier arriving (lighter) ion cannot detect higher mass ions from the same laser shot. Since all five peptides originated from the same area, they will invariably strike the same pixels as lower m/z ions. Figure 1e shows the integrated impact positions of the lightest peptide bradykinin fragment 1−7 (marked in red in Figure 1a). The grid structure is well-resolved in the ion distributions reaching the detector. By contrast, the ion counts of the heavier substance P ions (marked in blue in Figure 1a) are not sufficient to fully elucidate spatial features (Figure 1f). However, it is observed that most detected substance P ion counts colocalize with the bradykinin fragment 1−7 signal.

Cryo-sections of a bait fish were used to evaluate the method for analysis of complex biological samples containing endogenous water as an IR−MALDI matrix. The boundary region of two organs (liver and stomach) was irradiated with the laser-spot covering area of both organs (Figure 2b). Figure 2a shows the respective integrated spectrum over the whole

dx.doi.org/10.1021/ac403421v | *Anal. Chem.* XXXX, XXX, XXX−XXX

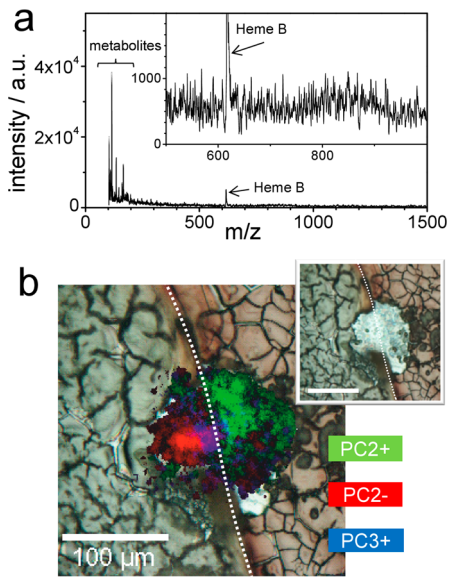

Figure 2. (a) IR–MALDI integrated mass spectrum of the liver (right) and stomach (left) region of a bait fish cryo-section without external matrix over all detector pixels from 2000 laser shots with some tentative assignments. (b) Overlay of a light microscopic image of the sample and the spatial distribution of the scores of PC2+ (green), PC2− (red), and PC3+ (blue) and light microscopic image of the section with burn mark left by IR irradiation (inset). The white dotted lines depict the boundary between the two organs.

detector from 2000 laser shots of the OPO laser system at 2.94 μm. Full ablation of the tissue was achieved after 2000−5000 laser shots.

The spectrum is dominated by intense peaks in the low mass region with low abundance ion signals up to 1500 Da observed. Reduced detection of ions with high m/z values could be caused by the single stop detection scheme of the TDC, as discussed above. Because of the low mass accuracy, mass resolution and lack of MS/MS capability, no definitive molecular assignments can be made. However, the origin of some peaks can be speculated. For example, in the low mass region (100−300 Da), small molecules, most likely metabolites, are detected, while a strong signal can be found at m/z 617.5. This can tentatively be assigned to protonated Heme B (MW: 616.48 Da), a precursor in the biosynthesis of hemoglobin, predominantly found in liver tissue.[28] A slight increase in the ion signal is observed in the m/z region typical for phospholipids (750−900 Da), but no precise m/z values can be assigned. Contrary to the here-presented high vacuum data, studies utilizing IR-MALDI on tissue at atmospheric pressure or rough vacuum find phospholipids to produce the most abundant peaks.[10] Although definitive molecular assignments are not possible, tissue-specific features can be extracted by performing principal component analysis (PCA) on the data to extract correlations among peaks on a pixel-by-pixel basis. To visualize these similarities, each pixel is assigned a score denoting its concordance with the principal component, with a high score accounting for high similarity. Figure 3b shows the positive (green) and negative (red) scores of PC2 and the positive score of PC3 (blue) overlaid on top of a light microscopic image of the irradiated sample (see inset for image without overlay and laser burn mark). It is apparent, that all three PCs group pixels of different tissue regions with the spatial distribution on the detector matching with the expected distribution based on light microscopy. It can be concluded that the mass spectrometric information loading PC2+ is characteristic for liver tissue, PC2- for stomach tissue, and PC3+ for the connective tissue in between. Full mass spectra of the three regions are shown in Figure 2 of the Supporting Information. All three regions show distinctively different ion signals. Tentatively assigned Heme B, for example, is found in the liver and the connective tissue with a much higher abundance than in the stomach. To our knowledge, this demonstrates for the first time the feasibility of IR-MALDI MS imaging in the microscope mode below the diffraction limit of the optical setup on a tissue slice using only endogenous water as a matrix.

CONCLUSION

We have shown that the combination of IR-excitation with microscope mode imaging utilizing a pixelated detector is a promising approach toward high-resolution molecular imaging without the requirements of an external matrix, bypassing the common optical limitations associated with use of long wavelength laser-light. While the method currently suffers from the single-stop nature of the TDC and the relatively wide time bins of the detector, developments in the Timepix detector design toward multistop TDC capabilities and enhanced time resolution could enable a more powerful exploitation of the mass spectra with respect to molecular identification and specificity, thereby making the method competitive with existing microprobe approaches. Nonetheless, in this proof-of-concept study, spatial features well below the diffraction limit of 14 μm were imaged with a pixel size of 766 nm and a spatial resolving power of 9.8 μm. In contrast to earlier IR-MALDI/stigmatic imaging studies, mass-resolved images could be acquired across a wide range of m/z values simultaneously. Furthermore, for the first time, the method was successfully implemented for untreated tissue slices utilizing the natural water content of the sample as a matrix.

ASSOCIATED CONTENT

Supporting Information

Additional information as noted in text. This material is available free of charge via the Internet at http://pubs.acs.org.

AUTHOR INFORMATION

Corresponding Author

*E-mail: heeren@amolf.nl.

Present Addresses

[§]Institute for Hygiene, University of Münster, Germany.
[∥]Paul Scherrer Institute, Villigen PSI, Switzerland.

Notes

The authors declare no competing financial interest.

ACKNOWLEDGMENTS

The authors thank the Institute of Hygiene of the University of Münster for the loan of an Er:YAG-Laser, Gert B. Eijkel for help with PCA analysis, and Bryn Flinders for tissue sectioning. This work was supported by a fellowship within the Postdoc Programme of the German Academic Exchange Service (DAAD) to J.S. Part of this research is supported by the Dutch Technology Foundation STW, which is the Applied Science Division of NWO, and the Technology Programme of the Ministry of Economic Affairs, Project OTP 11956. This work was part of the research programme of the Foundation for

Fundamental Research on Matter (FOM), which is part of The Netherlands Organization for Scientific Research (NWO).

REFERENCES

(1) Caprioli, R. M.; Farmer, T. B.; Gile, J. *Anal. Chem.* **1997**, *69*, 4751−4760.
(2) Spengler, B.; Hubert, M. *J. Am. Soc. Mass Spectrom.* **2002**, *13*, 735−748.
(3) Guenther, S.; Koestler, M.; Schulz, O.; Spengler, B. *Int. J. Mass Spectrom.* **2010**, *294*, 7−15.
(4) Schwartz, S. A.; Reyzer, M. L.; Caprioli, R. M. *J. Mass Spectrom.* **2003**, *38*, 699−708.
(5) Berkenkamp, S.; Menzel, C.; Karas, M.; Hillenkamp, F. *Rapid Commun. Mass Spectrom.* **1997**, *11*, 1399−1406.
(6) Pirkl, A.; Soltwisch, J.; Draude, F.; Dreisewerd, K. *Anal. Chem.* **2012**, *84*, 5669−5676.
(7) Dreisewerd, K.; Draude, F.; Kruppe, S.; Rohlfing, A.; Berkenkamp, S.; Pohlentz, G. *Anal. Chem.* **2007**, *79*, 4514−4520.
(8) Ibáñez, A. J.; Scharte, J.; Bones, P.; Pirkl, A.; Meldau, S.; Baldwin, I. T.; Hillenkamp, F.; Weis, E.; Dreisewerd, K. *Plant Methods* **2010**, *6*, 14−30.
(9) Li, Y.; Shrestha, B.; Vertes, A. *Anal. Chem.* **2007**, *79*, 523−532.
(10) Römpp, A.; Schäfer, K. C.; Guenther, S.; Wang, Z.; Köstler, M.; Leisner, A.; Paschke, C.; Schramm, T.; Spengler, B. *Anal. Bioanal. Chem.* **2013**, *405*, 6959−6968.
(11) Shrestha, B.; Vertes, A. *Anal. Chem.* **2009**, *81*, 8265−8271.
(12) Luxembourg, S. L.; Mize, T. H.; McDonnell, L. A.; Heeren, R. M. A. *Anal. Chem.* **2004**, *76*, 5339−5344.
(13) Llopart, X.; Ballabriga, R.; Campbell, M.; Tlustos, L.; Wong, W. *Nucl. Instrum. Methods Phys. Res., Sect. A* **2007**, *581*, 485−494.
(14) Jungmann, J. H.; MacAleese, L.; Visser, J.; Vrakking, M. J. J.; Heeren, R. M. A. *Anal. Chem.* **2011**, *83*, 7888−7894.
(15) Ellis, S. R.; Jungmann, J. H.; Smith, D. F.; Soltwisch, J.; Heeren, R. M. A. *Angew. Chem., Int. Ed.* **2013**, *125*, 11471−11474.
(16) Jungmann, J. H.; Heeren, R. M. A. *J. Proteomics* **2012**, *75*, 5077−5092.
(17) Jungmann, J. H.; MacAleese, L.; Buijs, R.; Giskes, F.; de Snaijer, A.; Visser, J.; Visschers, J.; Vrakking, M. J. J.; Heeren, R. M. A. *J. Am. Soc. Mass Spectrom.* **2010**, *21*, 2023−2030.
(18) Kiss, A.; Jungmann, J. H.; Smith, D. F.; Heeren, R. M. A. *Rev. Sci. Intrum.* **2013**, *84*, 013704.
(19) Jungmann, J. H.; Smith, D. F.; MacAleese, L.; Klinkert, I.; Visser, J.; Heeren, R. M. A. *J. Am. Soc. Mass Spectrom.* **2012**, *23*, 1679−1688.
(20) Luxembourg, S. L.; McDonnell, L. A.; Mize, T. H.; Heeren, R. M. A. *J. Proteome Res.* **2005**, *4*, 671−673.
(21) Jungmann, J. H.; Smith, D. F.; Kiss, A.; MacAleese, L.; Buijs, R.; Heeren, R. M. A. *Int. J. Mass Spectrom.* **2013**, *341−342*, 34−44.
(22) Turecek, D.; Holy, T.; Jakubek, J.; Pospisil, S.; Vykydal, Z. *J. Instrum.* **2011**, *6*, C01046.
(23) Mannschke, L. P. *Proc. SPIE* **1986**, *0584*, 278−282.
(24) Stutz, J.; Platt, U. *Appl. Opt.* **1997**, *36*, 1105−1115.
(25) Kampmeier, J.; Dreisewerd, K.; Schürenberg, M.; Strupat, K. *Int. J. Mass Spectrom.* **1997**, *169*, 31−41.
(26) Soltwisch, J.; Berkenkamp, S.; Dreisewerd, K. *Rapid Commun. Mass Spectrom.* **2008**, *22*, 59−66.
(27) Colliver, T. L.; Brummel, C. L.; Pacholski, M. L.; Swanek, F. D.; Ewing, A. G.; Winograd, N. *Anal. Chem.* **1997**, *69*, 2225−2231.
(28) Shimma, S.; Sugiura, Y.; Hayasaka, T.; Zaima, N.; Matsumoto, M.; Setou, M. *Anal. Chem.* **2008**, *80*, 878−885.